Demonstration of a Symmetric 10 Gb/s QPSK Subcarrier Multiplexed WDM PON with IM/DD Transceivers and a Bandwidth-limited RSOA

J. M. Buset,[1,*] Z. A. El-Sahn,[1,2] and D. V. Plant[1]

[1] Photonics Systems Group, Department of Electrical and Computer Engineering,
McGill University, Montréal, QC H3A 2A7, Canada.
[2] Electrical Engineering Department, Alexandria University, Alexandria 21544, Egypt.

[*] jonathan.buset@mail.mcgill.ca

Abstract: Full-duplex 10 Gb/s/λ transmission is demonstrated over a 20 km single feeder WDM PON. BER performance below the RS(255,223) FEC threshold is achieved for OLT launch powers, ranging from 0 dBm to 9 dBm, proving flexibility to network operators.

© 2012 Optical Society of America

OCIS codes: (060.0060) Fiber optics and optical communications; (060.2330) Fiber optics communications;

1. Introduction

Access networks must continue to evolve to meet increasing consumer demand for high bandwidth services such as streaming Internet video, 3-D television, video-on-demand and cloud-based storage [1]. These popular data intensive services will drive adoption of fiber-to-the-home (FTTH) to meet the need for greater capacity on access networks.

Future passive optical networks (PONs) using time-division multiplexing (TDM), such as 10G-EPON and XG-PON, will provide a short term upgrade pathway for operators to increase the total shared bandwidth available to users, but scaling TDM-based networks beyond 10 Gb/s is expected to be technically challenging [2]. In the long term, wavelength-division multiplexing (WDM) in PONs is expected to provide the additional bandwidth needed to achieve these performance goals. Viable WDM solutions will require single feeder architectures and colourless optical network units (ONUs) to maintain compatibility with existing deployed infrastructure while reducing inventory redundancy.

In recent years, digital signal processing (DSP) has proven to be an effective technique in next generation transport network systems by replacing expensive optical components with high-speed transceiver electronics [3]. There is great potential for access networks to build upon these signal processing techniques using lower speed electronic components to achieve significant performance increases from economical optoelectronic transmitters.

This paper demonstrates the performance of a new WDM PON with symmetric transmission at 10 Gb/s per wavelength using commodity intensity modulation (IM)/direct detection (DD) transceivers and bidirectional transmission on the same wavelength. DSP spectral pre-compensation, offset optical filtering and electronic equalization are used to compensate for the bandwidth-limited reflective semiconductor optical amplifier (RSOA) ONU transmitter. Leveraging transport network DSP techniques, this architecture transmits QPSK modulated data signals for the uplink and downlink that are subcarrier multiplexed (SCM) on different frequencies in the electrical domain. This provides robust resistance to the effects of in-band noise due to reflections and Rayleigh backscattering [4], allowing operation over a wide range of launch powers from 0 dBm to 9 dBm. To the best of our knowledge, this is the first demonstration of a symmetric 10 Gb/s WDM PON with wavelength re-use and QPSK transmission using IM/DD for both the uplink and downlink directions.

2. DSP enabled SCM WDM PON

2.1. PON physical architecture

The single feeder architecture used in this experiment is illustrated in Fig. 1. The optical line terminal (OLT) transmitter consists of a Micram VEGA digital-to-analog converter (DAC) with 6 bit precision driving an electro-absorption modulated laser (EML) centred at 1549.57 nm. Following the EML, a booster EDFA and VOA control the launch power P_{Tx}. The optical distribution network (ODN) comprises a 20.35 km feeder of standard single mode fiber (SMF-28e+), a 100 GHz arrayed waveguide grating (AWG) and a 1.5 km distribution drop fiber (DDF). At the ONU, an optimized

coupler taps off 80% of the downstream signal for detection by the receiver comprised of a p-i-n photoreceiver, a RF amplifier, and a real-time oscilloscope performing analog-to-digital conversion (ADC). The remaining 20% of the downstream signal seeds a RSOA with peak gain from 1530 nm to 1570 nm and ~ 2 GHz modulation bandwidth. The RSOA uplink transmitter is directly modulated at 4 V_{p-p}, biased at 80 mA, and driven by a second VEGA DAC. The OLT receiver consists of a 0.25 nm tuneable optical band pass filter (OBPF), a pre-amp EDFA and VOA to fix the received power at -2 dBm, along with a p-i-n photoreceiver, RF amplifier and ADC to capture the received signal. In addition to the DSP pre-compensation, the effective uplink bandwidth is further increased by offsetting the centre of the OBPF from the peak upstream wavelength by an optimized $\Delta\lambda = -0.07$ nm [5].
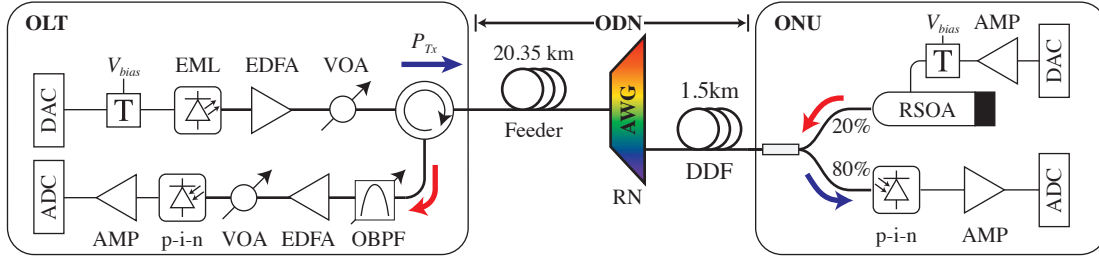
Fig. 1. Physical architecture of the proposed SCM WDM PON. AMP: RF amplifier, EDFA: erbium-doped fiber amplifier, RN: remote node, T: RF bias-tee, VOA: variable optical attenuator.

2.2. *Software enabled DSP transceivers*

A general flow outline of the transmitter and receiver software stacks used in this experiment are illustrated in Fig. 2. For the transmitters, $2^{23} - 1$ and $2^{31} - 1$ length pseudo-random bit sequences (PRBSs) are first generated respectively for the downlink and uplink. A short ~ 2 kbit preamble is added to the beginning of each PRBS and the entire sequence is truncated to a length of 256 kbit due to DAC memory limitations. After QPSK symbol mapping, a root raised cosine (RRC) filter is then applied to increase the spectral efficiency and reduce the effects of inter-symbol interference (ISI). The signal is then upsampled and multiplexed on a RF subcarrier f_{sc}. An additional pre-compensation filter, approximating the inverse of the transmitter's modulation response, is applied to boost the high frequency components and compensate for the bandwidth roll-off. The VEGA DACs then transmit the quantized data at 5 Gbaud.
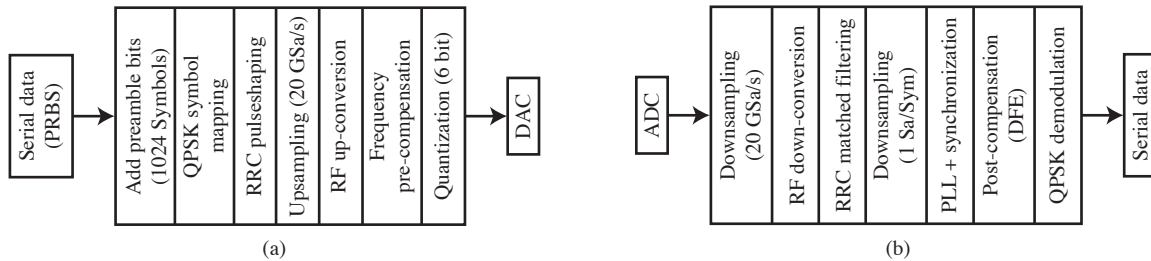
Fig. 2. Generalized block diagrams of the (a) transmitter and (b) receiver DSP stacks used for uplink and downlink transmission.

At the receivers, the captured 40 GSa/s data is downsampled, RF down-converted, and a matching RRC filter is applied to eliminate ISI and the remove out-of-band noise. After synchronization and QPSK decision blocks, the short preamble is used to remove the PLL phase ambiguity and then to train a post-compensation decision feedback equalizer (DFE) comprising 4 forward and 1 backward symbol-spaced taps. After training, the DFE taps are dynamically adjusted using the least-mean square (LMS) algorithm. This DFE removes any residual ISI that may have occurred through propagation. After post-compensation, the QPSK signal is demodulated for bit-error ratio (BER) calculation.

3.   **Experimental results & discussion**

In Fig. 3(a), we illustrate the power spectral density (PSD) of the captured data sequences. The downlink signal is centred at $f_{sc\_DL} = 7.66$ GHz with a RRC roll-off factor of $\alpha_{DL} = 0.35$. At high frequencies the flatness of the

downlink band becomes distorted primarily by the 10 GHz receiver bandwidth. The uplink spectrum, with a roll-off factor of $\alpha_{UL} = 0.15$ and a $f_{sc\_UL} = 2.97$ GHz carrier, maintains a flat response throughout the band due to the DSP pre-compensation and offset optical filtering. The uplink spectrum overlaps with the reflected downlink by ~ 1.5 GHz.

A study of the system BER as a function of launch power P_{Tx} is demonstrated in Fig. 3(b) and (c) for symmetric QPSK transmission at 5 Gbaud (10 Gb/s). The BER is calculated using $\sim 4 \times 10^6$ bit of data, and after equalization both the downlink and uplink transmissions achieve a BER below the Reed-Solomon (RS) FEC threshold at $P_{Tx} \geq$ 0 dBm. This assumes that for RS(255,223), an undecoded BER of 1.1×10^{-3} is required to achieve a decoded BER of 1×10^{-12} [6]. Furthermore the performance is sustained up to $P_{Tx} = 9$ dBm, demonstrating this system's resistance to upstream impairments, such as Rayleigh backscattering and reflections, which are exacerbated by high launch powers.
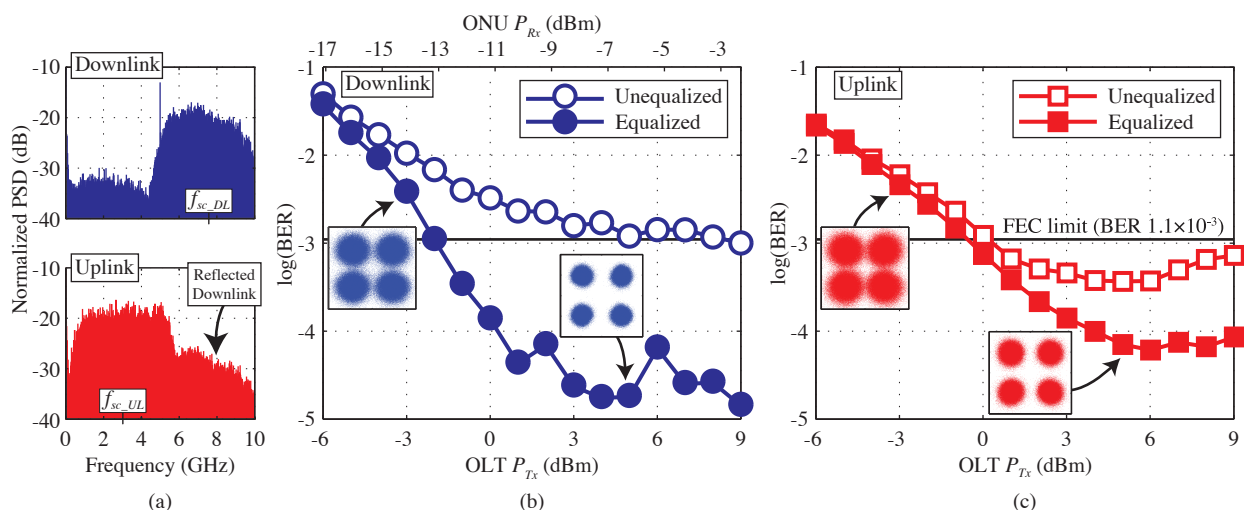
Fig. 3. (a) The electrical spectra of the received data captured at $P_{Tx} = 5$ dBm. BER performance of the (b) downlink and (c) uplink transmissions after 20 km. Constellation diagrams after electronic equalization at -3 dBm and 5 dBm are inset as indicated. The corresponding received power P_{Rx} for the downlink signal is also included for completeness. P_{Rx} for the uplink is fixed at -2 dBm.

This proposed solution provides a number of advantages that are attractive to network operators. Using a simple wavelength re-use scheme and IM/DD transceivers at both the OLT and ONU simplifies the optoelectronic requirements, eliminating the need for a local oscillator as in coherent PON solutions [7, 8]. It also provides higher bit rates and greater spectral efficiency than previous SCM WDM PONs using OOK modulation [9]. Finally, the wide range of operating launch powers provides additional flexibility to network operators, and the low $P_{Tx} \geq 0$ dBm operating point will help reduce the PON's energy footprint and operating costs. Additional research may further improve the system's performance by enabling the use of higher order modulation formats and/or more aggressive pulse shaping.

4. Conclusion

In this paper we demonstrate a new single feeder 10 Gb/s QPSK SCM WDM PON architecture that maximizes the performance of low cost IM/DD optoelectronics using DSP techniques. We verify the system's full-duplex performance over 20 km and achieve BERs below the RS(255,223) FEC threshold over a wide range of launch powers from 0 dBm to 9 dBm. To the best of our knowledge this is the highest symmetric bit rate reported for a WDM PON with wavelength re-use and IM/DD QPSK transmission for both the uplink and downlink directions.

References

1. "Cisco Visual Networking Index: Forecast and Methodology, 2010–2015," Tech. rep., Cisco Inc. (2011).
2. D. Breuer, et al., ITG (2011), paper 12.
3. K. Roberts, et al., IEEE Commun. Mag. **48**, 62–69 (2010).
4. C. Arellano, et al., JLT **27**, 12–18 (2009).
5. I. Papagiannakis, et al., PTL **20**, 2168–2170 (2008).
6. K. Tanaka, et al., JLT **28**, 651–661 (2010).
7. S.-Y. Kim, et al., OFC (2009), paper OTuH4.
8. N. Cvijetic, JLT **30**, 384–398 (2012).
9. J. M. Buset, et al., OE **20**, 14428–14436 (2012).